FEBS Letters 580 (2006) 2109–2116

An *Arabidopsis* SBP-domain fragment with a disrupted C-terminal zinc-binding site retains its tertiary structure

Kazuhiko Yamasaki[a,b,*], Takanori Kigawa[b,c], Makoto Inoue[b], Tomoko Yamasaki[a], Takashi Yabuki[b], Masaaki Aoki[b], Eiko Seki[b], Takayoshi Matsuda[b], Yasuko Tomo[b], Takaho Terada[b,d], Mikako Shirouzu[b,d], Akiko Tanaka[b], Motoaki Seki[e,f], Kazuo Shinozaki[e,f,g], Shigeyuki Yokoyama[b,d,h]

[a] *Age Dimension Research Center, National Institute of Advanced Industrial Science and Technology (AIST), 1-1-1 Higashi, Tsukuba 305-8566, Japan*
[b] *Protein Research Group, RIKEN Genomic Sciences Center, 1-7-22 Suehiro-cho, Yokohama 230-0045, Japan*
[c] *Department of Computational Intelligence and Systems Science, Interdisciplinary Graduate School of Science and Engineering, Tokyo Institute of Technology, 4259 Nagatsuta-cho, Midori-ku, Yokohama 226-8503, Japan*
[d] *RIKEN SPring-8 Center, Harima Institute, 1-1-1 Kouto, Sayo, Hyogo 679-5148, Japan*
[e] *Plant Functional Genomics Research Group, RIKEN Genomic Sciences Center, 1-7-22 Suehiro-cho, Tsurumi-ku, Yokohama 230-0045, Japan*
[f] *Laboratory of Plant Molecular Biology, RIKEN Tsukuba Institute, 3-1-1 Koyadai, Tsukuba 305-0074, Japan*
[g] *RIKEN Plant Science Center (PSC), RIKEN Yokohama Institute, 1-7-22 Suehiro-cho, Tsurumi-ku, Yokohama 230-0045, Japan*
[h] *Department of Biophysics and Biochemistry, Graduate School of Science, The University of Tokyo, 7-3-1 Hongo, Bunkyo-ku, Tokyo 113-0033, Japan*

Received 22 December 2005; revised 3 March 2006; accepted 5 March 2006

Available online 20 March 2006

Edited by Christian Griesinger

Abstract ***SQUAMOSA*** **promoter-binding proteins (SBPs) form a major family of plant-specific transcription factors, mainly related to flower development. SBPs share a highly conserved DNA-binding domain of ~80 amino acids (SBP domain), which contains two non-interleaved zinc-binding sites formed by eight conserved Cys or His residues. In the present study, an** ***Arabidopsis*** **SPL12 SBP-domain fragment that lacks a Cys residue involved in the C-terminal zinc-binding pocket was found to retain a folded structure, even though only a single Zn^{2+} ion binds to the fragment. Solution structure of this fragment determined by NMR is very similar to the previously determined structures of the full SBP domains of** ***Arabidopsis*** **SPL4 and SPL7. Considering the previous observations that chelating all the Zn^{2+} ions of SBPs resulted in the complete unfolding of the structure and that a mutation of the Cys residue equivalent to that described above impaired the DNA-binding activity, we propose that the Zn^{2+} ion at the N-terminal site is necessary to maintain the overall tertiary structure, while the Zn^{2+} ion at the C-terminal site is necessary for the DNA binding, mainly by guiding the basic C-terminal loop to correctly fit into the DNA groove.**

Keywords: Zinc binding; Transcription factor; Protein–DNA interaction; *Arabidopsis thaliana*

1. Introduction

The *SQUA*-promoter binding proteins (SBPs) are putative plant-specific transcription factors. SBPs were originally identified in *Antirrhinum majus* as the factors that bind to the promoter DNA of the floral meristem identity gene *SQUAMOSA* [1]. *A. majus* SBP1 and SBP2 are related to the control of flower development, as they possess primary structures characteristic of the transcriptional activator, and are expressed prior to the *SQUAMOSA* gene. In *Arabidopsis*, 16 SBPs were identified, termed *SQUAMOSA* promoter binding protein-like (SPL) proteins [2]. To date, functions of only a few *Arabidopsis* SBPs were reported; SPL3 is considered to be the orthologue of the *A. majus* SBPs and the plants with constitutive overexpression of SPL3 showed an early flowering phenotype [3]; SPL8 is required for pollen sac development [4]; and SPL14 is related to sensitivity to a fungal toxin as well as leaf morphology [5].

SBPs are diverse in the primary structures although they share a highly conserved DNA-binding domain of ~80 amino acids in length, termed SBP domain [2]. Previously, we have determined the solution structures of the SBP domains of *Arabidopsis* SPL4 and SPL7 proteins [6]. The structure of the SBP domain contains two zinc-binding sites consisting of eight Cys or His residues in a $Cys_3HisCys_2HisCys$ (or $Cys_6HisCys$ in minority) sequence motif of a non-interleaved coordination manner – i.e., the first four residues coordinate to one Zn^{2+} ion (the N-terminal or "first" site, in the present manuscript) and the last four coordinate to the other (the C-terminal or "second" site in the present manuscript). This is dissimilar to other known zinc-binding structures, and thus represented a novel type of zinc-binding motif.

The functions of the two individual Zn^{2+} ions were unknown. It was reported by other groups that simply adding chelating reagent, EDTA or *o*-phenanthroline, does not reduce the DNA-binding activities of *A. majus* SBPs and *Arabidopsis* SPL1 and SPL14 [1,5,7]. On the other hand, we have observed that EDTA added to the solutions of *Arabidopsis* SPL4 and SPL7 proteins chelates out the two bound Zn^{2+} ions and unfolds the protein structures [6]. Consistently, an analysis including unfolding–refolding process revealed that chelating the Zn^{2+} ions results in the disruption of DNA-binding activity of *Arabidopsis* SPL1 [7]. It was also demonstrated in the same report that a mutation of one of the conserved Cys/His

*Corresponding author. Fax: +81 29 861 2706.
E-mail address: k-yamasaki@aist.go.jp (K. Yamasaki).

0014-5793/$32.00 © 2006 Published by Elsevier B.V. on behalf of the Federation of European Biochemical Societies.
doi:10.1016/j.febslet.2006.03.014

residues that form the second binding pocket impaired the DNA-binding activity of *Arabidopsis* SPL1, although a mutation of another residue of the same binding pocket resulted in only a partial impairment [7].

In the present study, in the process of selecting the shortest fragment for the NMR structural determination, an *Arabidopsis* SPL12 fragment that lacks one of the zinc-coordinating residues were found to be folded. Indeed, the determined structure was very similar to the previously determined SBP structures of *Arabidopsis* SPL4 and SPL7. Considering the previous observations, the difference in the functions of the two bound Zn^{2+} ions were elucidated.

2. Methods

2.1. Sample preparation

The DNAs that code for SBP-domain fragments of SPL12 (Ala124-Asp215, Ala124-Thr205, and Ala124-Asp181 corresponding to 1–92, 1–82, and 1–58, respectively, by the numbering scheme in the SBP-domain alignment in Fig. 1A and Refs. [6,7], which will be used hereafter in the present manuscript) were subcloned into pCR2.1 vector (Invitrogen) by PCR from an *Arabidopsis* full-length cDNA clone with ID RAFL09-41-M16 (MIPS code: At3g60030) [8]. The PCR primers used were designed so that the T7 promoter sequence, ribosome-binding site, and oligohistidine tag, as well as the cleavage site for tobacco etch virus (TEV) protease are attached at the 5′ end, and that the T7 terminator sequence is attached at the 3′ end (T. Yabuki, Yoko Motoda, Miyuki Saito, Natsuko Matsuda, T.K. and S.Y., unpublished results). Consequently, additional amino acids, GlySer, derived from the expression vector were attached to the N-terminus. The ^{15}N-labeled and unlabeled proteins were expressed by a large-scale cell-free system developed in RIKEN [9–11]. The reaction mixture was supplemented with 50 μM $ZnCl_2$. The proteins were purified by a HisTrap™ (Amersham) column or a combination of TALON™ (Clontech) and HiTrap™ SP (Amersham) columns. The buffers used were [20 mM Tris–HCl (pH 8.0), 0.3–1 M NaCl, 20–500 mM imidazole, 50 μM $ZnCl_2$, and 1 mM iminodiacetic acid] for HisTrap™ chromatography, [20 mM Tris–HCl (pH 7.0), 300–750 mM NaCl, 0–500 mM imidazole, and 50 μM $ZnCl_2$] for TALON™ chromatography, and [20 mM Tris–HCl (pH 7.0), 0–1 M NaCl, 50 μM EDTA, 100 μM $ZnCl_2$, and 1 mM dithiothreitol (DTT)] for HiTrap™ SP chromatography. Protein concentration was determined by A_{280} values and molar absorption coefficients calculated from the amino-acid sequences. For estimation of folding by NMR measurements, 0.3–0.4 mM ^{15}N-labeled proteins were dissolved in 20 mM Tris–HCl buffer (pH 7.5) containing 300 mM NaCl, 50 μM EDTA, 100 μM $ZnCl_2$, 5 mM DTT, and 10% D_2O or sodium phosphate buffer (pH 6.0) containing 300 mM NaCl, 20 μM $ZnCl_2$, and 10% D_2O. For structure determination by NMR, ~1.0 mM unlabeled protein (Ala1-Asp58) was dissolved in 20 mM potassium phosphate buffer (pH 6.0) containing 300 mM KCl, 20 μM $ZnCl_2$, 1 mM deuteriated DTT (Isotec Inc.), 0.5 mM sodium 2,2-dimethyl-2-silapentane-5-sulfonate (DSS), and 5% D_2O. For circular dichroism (CD) titration experiments, proteins of an initial concentration of 0.12 mM were dissolved in 20 mM potassium phosphate buffer (pH 5.5 or 6.0) or 20 mM Tris–HCl buffer (pH 7.5), containing 300 mM KCl, 20 μM $ZnCl_2$, and 1 mM DTT.

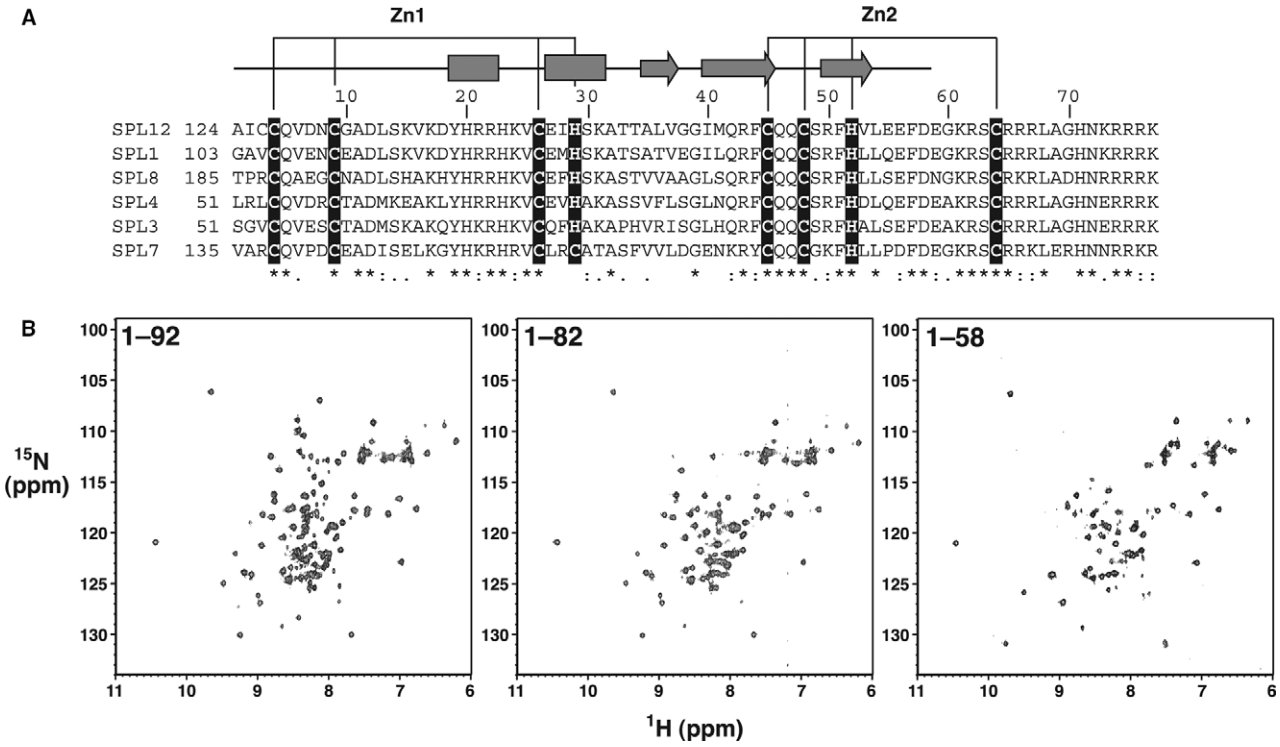

Fig. 1. (A) Sequence alignment of the SBP domains of *Arabidopsis* SPL proteins produced by the Clustal X program [20]. SPL proteins from the "Columbia" cultivar appearing in the NCBI database (http://www.ncbi.nlm.nih.gov) were selected: SPL1 (CAB56580), SPL3 (CAB56579), SPL4 (CAB56582), SPL7 (CAB56575), SPL8 (CAB56593), and SPL12 (CAB56768). Numbers above the sequences are for the present alignment of the SBP domain and are used in the text, while those of the first residues of the aligned sequences of the individual proteins are indicated beside the sequences. The Cys or His residues involved in the zinc binding [6] are reversely shown in the black boxes. Boxes and arrows above the sequence indicate regions of helices and strands, respectively, of the structure of SPL12-trSBP (Ala1-Asp58), accompanied by a horizontal line showing the region of the fragment. Two quartettes of the zinc-coordinating residues are connected by lines, although the second one is not indeed formed in SPL12-trSBP. Below the sequence, identical and similar residues are marked according to the definition in the program. (B) ^{1}H–^{15}N HSQC spectra of three SPL12-SBP fragments of different lengths. Regions of the fragments are shown in the spectra by amino acid numbers used for the SBP domain alignment as in (A).

2.2. CD measurements and analyses

CD spectra were recorded on a JASCO J-820 spectropolarimeter at 298 K, as described previously [6]. Titration experiments were conducted by adding increasing amounts of 3 mM EDTA. Before starting the titration of EDTA, initially existing Zn^{2+} ion (20 μM) was chelated out by adding the same amount of EDTA. The changes in ellipticity were fitted to either of two theoretical models by in-house FORTRAN programs that employ a nonlinear least-squares method of the IMSL subroutine library (IMSL Inc.). Namely, one model is that the simultaneous binding of two Zn^{2+} ions to a protein molecule competes the binding of a Zn^{2+} ion and EDTA, where a Zn^{2+}/EDTA binding constant of 3.2×10^{16} M^{-1} [12] was used. Error level in the obtained binding constant of the protein and Zn^{2+} ions was estimated by a Monte Carlo approach where the initial fitting residuals in the CD value was employed as the standard deviation of the Gaussian distribution, by using an IMSL subroutine. The other model is that the binding of the Zn^{2+} ion to the protein is not strong enough to compete the Zn^{2+}/EDTA binding, resulting in a linear line with a saturation value.

2.3. NMR measurements, resonance assignments, and structural calculation

For the initial estimation of folding, ^{1}H–^{15}N HSQC spectra of different SBP-domain fragments were recorded on a Bruker AVANCE 600 spectrometer (600.18 MHz for ^{1}H and 60.82 MHz for ^{15}N) at 298 K. For structure determination, typical homonuclear NMR spectra [13] of the shortest fragment (Ala1-Asp58) were recorded on a Bruker DMX-750 (750.13 MHz for ^{1}H) spectrometer at 293 K, essentially as previously described [6]. The recorded spectra were analyzed for the backbone and side chain resonances assignments, also as described previously [6].

Distance constraints derived from a NOESY spectrum, $\chi 1$ angle constraints for stereo-specifically assigned residues, and theoretical constraints for the Zn^{2+} coordination were imposed as described [6]. Random simulated annealing [14] was carried out by using the program CNS [15], also as described [6]. The co-ordinates of the structure of the SPL12-trSBP were deposited to the Protein Data Bank under accession ID 1WJ0.

2.4. Surface plasmon resonance

Experiments were carried out at 298 K using a Biacore X apparatus (BIACORE). The running buffer was 20 mM potassium phosphate (pH 6.0) containing 100–300 mM KCl, 20 μM $ZnCl_2$, and 0.005% Tween 20. A total of 594 and 580 resonance unit (RU) of two double-stranded DNAs [5′-bio-GACGTCCGTACAACAAG-3′/5′-CTTGTTGTACGGACGTC-3′; the consensus sequence of the SBP-binding sites [2] is underlined, and "bio" stands for biotinylation] and [5′-bio-GGGCATTTATCTTGAATC-3′/5′-GATTCAAGATAAATGCCC-3′], respectively, were immobilized on the surfaces of Sensor Chip SA (Biacore) in one (flow cell 2) of the two flow cells, so that the other is treated as the control to be subtracted. Protein solutions at the concentration range of 5 nM to 1 μM, were injected into the flow cells at 5–20 μL min^{-1} for 5–20 min. For sensorgrams that did not reach equilibrium within the durations, especially at low protein concentrations, injection was repeated successively until they reach equilibrium, or the data was not used for the calculation of the binding constants. The relations between the equilibrium response values and the protein concentrations were fitted to the simple 1:1 binding model by using BIAevaluation 3.0 software (Biacore) to obtain the equilibrium binding constants.

3. Results and discussion

3.1. Selection of the shortest fragment for NMR structure determination

For structure determination of protein domains, selection of the smallest, correctly folded fragment is one of the key steps. In this process, we have prepared several fragments with different length including the SBP domain (Ala1-Lys77) at least partially and evaluated their folding by NMR measurements (Fig. 1). Among the three NMR spectra shown in Fig. 1B, those of the longer two fragments (left and middle) are very similar to each other, except that the longest possesses more cross-peaks in the central region of the spectra probably corresponding to unstructured region(s). The spectrum of the shortest one, Ala1-Asp58, still showed cross-peaks well spread in the spectrum, reflecting a large chemical shift dispersion, and is largely similar to the other two. This indicates that it possesses specific tertiary structure similar to the longer fragments. This was somewhat surprising because this shortest fragment lacks Cys64, which is one of the conserved Cys/His residues forming the second zinc-binding pocket, and because we previously observed that chelating the bound Zn^{2+} ions from similar *Arabidopsis* SPL4 and SPL7 SBP domains resulted in the structural unfolding [6]. In the present study, we have selected this shortest fragment for the structure determination target and termed it SPL12-trSBP (truncated SBP) in the present manuscript. We also use fragment 1–82 that includes the whole SBP domain as control and termed it SPL12-flSBP (full-length SBP).

3.2. Bound Zn^{2+} ions of SPL12-SBP fragments

In the previous report, we have shown by the far-UV CD and NMR measurements that the SBP domains of *Arabidopsis* SPL4 and SPL7 each contain two bound Zn^{2+} ions and that chelating of the Zn^{2+} ions leads to structural unfolding [6]. In the present study, we analyzed bound Zn^{2+} ions of the SPL12-SBP fragments also by far-UV CD spectroscopy (Fig. 2). The CD spectrum of SPL12-flSBP is similar to that of SPL4-SBP in that they possess a positive peak at ~220 nm (Fig. 2A; Ref. [6]). By adding EDTA to the protein solutions at pH 5.5 or 6.0, spectral changes were observed (Fig. 2A and B). The change appears to finish approximately at the 1:2 molar ratio of protein and EDTA for the solution at pH 5.5 (Fig. 2A and B), revealing that Zn^{2+} ions of twofold the proteins were released. It is important to note that the change of CD up to the 1:2 molecular ratio is almost linear, which is also the case with *Arabidopsis* SPL4 and SPL7 [6]. This indicates a two-state transition scheme in which two Zn^{2+} ions are simultaneously released from the protein – i.e., although an intermediate state containing a single Zn^{2+} ion could be assumed, its fraction is negligible, probably because it is much less stable than that contains two Zn^{2+} ions. Indeed, the change in the CD of solution at pH 6.0 was successfully fit to the model that simultaneous binding of two Zn^{2+} ions by the protein competes binding of a Zn^{2+} ion by EDTA (see Section 2.2). The estimated protein–Zn^{2+} binding constant is $3.7(\pm 2.2) \times 10^{31}$ M^{-2}, when the EDTA–Zn^{2+} binding constant of 3.2×10^{16} M^{-1} [12] was employed for the calculation. As the protein–Zn^{2+} binding constant would be 1.0×10^{33} M^{-2} if both the binding constants of the individual sites are the same as that of the EDTA–Zn^{2+} binding, it was indicated that the protein binds to Zn^{2+} ions less strongly than EDTA by ~30-fold at pH 6.0.

In contrast to these, the CD value was not significantly changed for solution at pH 7.5 (Fig. 2B). The above difference in the behaviors at different pH is likely to be due to the pH-dependence of the structural stability of the SBP domain, which should be related to the pK_a value of His side-chain, 6.04 [16]. Namely, at pH lower than 6.0, His side-chain has stronger tendency to be positively charged, which destabilize its coordination to a Zn^{2+} cation by the electrostatic repulsion. Consequently, protein–Zn^{2+} binding is extremely weaker than EDTA–Zn^{2+} binding at pH 5.5, whereas it is ~30-fold weaker

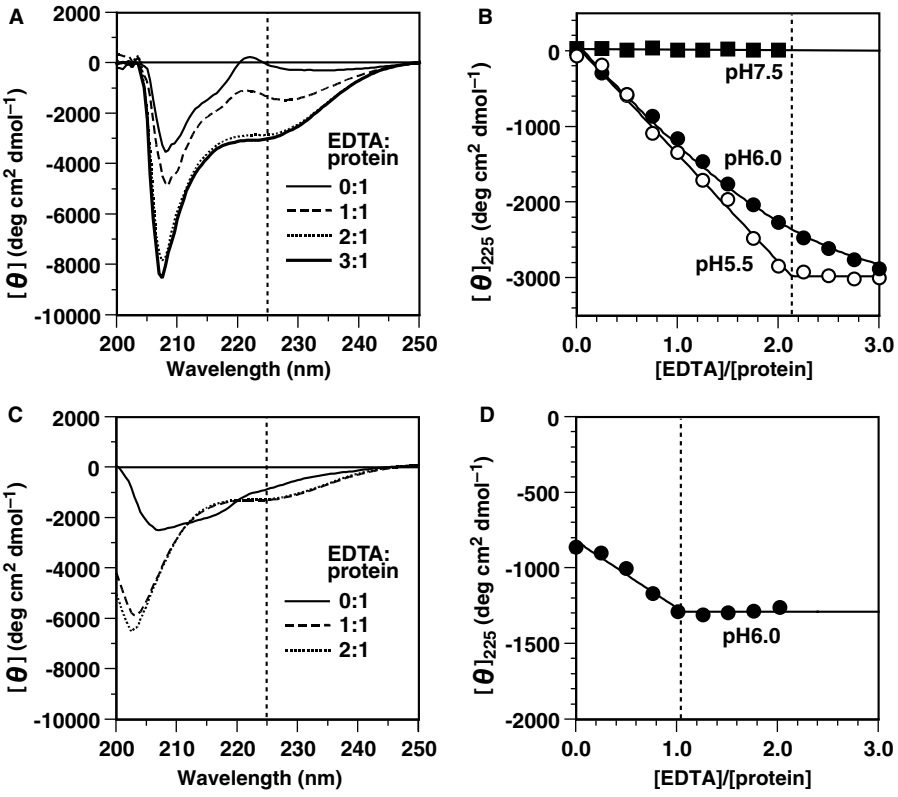

Fig. 2. Bound zinc ions analyzed by circular dichroism (CD). (A) CD spectra of SPL12-flSBP (Ala1-Thr82) in the absence (thinner solid line) or presence of an equivalent amount (dashed line), twofold excess (dotted line) or threefold excess (bold solid line) of EDTA, measured at pH 5.5 are shown. (B) The change in the CD value was monitored at 225 nm, which is marked by a dotted vertical line in (A), during the titration of EDTA at pH5.5 (open circles), 6.0 (closed circles), or 7.5 (closed squares). Solid lines in (B) indicate linear or nonlinear least-squares theoretical fitting curves: a linear change of ellipticity up to a saturation value (pH 5.5), a model in which two ions simultaneously bind to a protein (pH 6.0) (see Section 2.2), and a simple linear line (pH 7.5). The point of the saturation for data at pH 5.5 is shown by a dotted vertical line. (C) CD spectra of SPL12-trSBP (Ala1-Asp58) in the absence (solid line) or presence of equivalent amount (dashed line) or twofold excess (dotted line) of EDTA, measured at pH6.0 are shown. (D) The change in the CD value during the titration of EDTA was monitored also at 225 nm, the position of which is marked by a dotted vertical line in (C). A solid line and a dotted vertical line in (D) indicate a linear change in the ellipticity up to a saturation value as fitted nonlinearly, and the point of saturation, respectively.

at pH 6.0, and extremely stronger at pH 7.5 (Fig. 2B). This is likely to explain the previous observation that EDTA or *o*-phenanthroline did not affect the DNA-binding activities of several SBPs [1,5,7]. Indeed, the gel retardation experiment of *Arabidopsis* SPL1 was performed at pH 7.5–8.0 [7], whereas our previous titration experiment on SPL4- and SPL7-SBPs was performed at pH 6.0 [6]. It should be noted that binding of Zn^{2+} ions by SPL12-SBP is likely to be significantly stronger than that by SPL4- or SPL7-SBP, since the previous titration experiment on SPL4- or SPL7-SBP at pH 6.0 showed linear change like SPL12-SBP at pH 5.5, indicating that its binding of Zn^{2+} ions is extremely weaker than EDTA [6].

The same experiment was performed for SPL12-trSBP at pH 6.0 (Fig. 2C and D). The change is smaller than SPL12-flSBP and appears to be complete nearly at the 1:1 molar ratio of protein and EDTA. Since the change is linear up to the saturation level, binding of a Zn^{2+} ion by SPL12-trSBP is extremely weaker than that by EDTA, and therefore significantly weaker than that by SPL12-flSBP.

From the observations described above, it is evident that SPL12-flSBP binds two Zn^{2+} ions, whereas SPL12-trSBP binds a single Zn^{2+} ion. That is, lack in Cys64 that forms the second zinc-binding site indeed disrupts the binding of a Zn^{2+} ion at this site.

3.3. Structural description of SPL12-trSBP

The solution structure of the SPL12-trSBP was determined by NMR, which satisfies the experimental constraints and possesses idealistic stereochemical properties (Table 1). Secondary structure elements are two short helices (Tyr19-Arg22 and Glu27-Lys31) and a three-stranded antiparallel β-sheet (Ala35-Val37, Ile40-Cys45, and Arg50-Val53), as identified by the program Procheck-NMR [17] (Figs. 1A, 3B). Also, the N-terminal loop region is folded similarly to an antiparallel β-sheet, in which two very short β-strands (Ile2-Cys3, Asp12-Leu13) were indeed identified for some of the selected structures by the same program. The above secondary structure elements and the N-terminal loop region were packed against each other by the zinc coordination at the first binding site and by hydrophobic interactions. Extensive hydrophobic interactions were observed between Ile2-Leu13, Ile2-Arg21, Ile2-Lys24, Gln5-Lys24, Val6-His29, Val6-Val37, Val6-Phe51, Val25-Phe44, Val25-Phe51, His29-Ala35, Val37-Gln42, Val37-Phe51, Gln42-Phe51, and His52-Phe57, as defined by more than two pairs of side-chain carbon atoms having average distances of <4.5 Å over the 20 structures of the ensemble (e.g., between Ile2 and Leu13, three carbon atom pairs, Ile2/CB-Leu13/CB, Ile2/CB-Leu13/CD1, and Ile2/CG2-Leu13/CD1, have distances <4.5 Å on average). It should be noted

Table 1
Structural statistics

Structural constraints		
Intraresidue NOEs	383	
Sequential NOEs	170	
Medium-range NOEs ($2 \leqslant \|i-j\| \leqslant 4$)	92	
Long-range NOEs ($\|i-j\| > 4$)	250	
Torsion ($\chi 1$) angles	19	
Theoretical[a]	14	
Total	928	
Structural characteristics	Ensemble of 20 structures	Minimized mean structure
R.m.s. deviation from constraints[b]		
NOEs and hydrogen bonds (Å)	0.0022 ± 0.0007	0.001
Torsion angles (°)	0.0015 ± 0.0063	0.000
van der Waals energy (kcal/mol)[c]	13.9 ± 0.4	13.0
R.m.s. deviation from the ideal geometry[b]		
Bond lengths (Å)	0.0008 ± 0.0000	0.0006
Bond angles (°)	0.284 ± 0.001	0.279
Improper angles (°)	0.094 ± 0.003	0.083
Average r.m.s. deviation from the unminimized mean structure[d]		
N, C_α, C	0.50 ± 0.05	
All heavy atoms	1.02 ± 0.06	
Ramachandran plot		
Most favored region (%)	67.1	69.8
Additionally allowed region (%)	30.4	28.3
Generously allowed region (%)	2.2	1.9
Disallowed region (%)	0.4	0.0

[a]Distance, angle, and plane restraints applied for Zn^{2+} ions and coordinating atoms (see Ref. [6]).
[b]Parameters related to the theoretical constraints are excluded.
[c]Values calculated with the force field for NMR structure determination in the CNS package.
[d]Values calculated with Ala1-Leu54.

that these include two zinc-coordinating His residues at the first site (His29) as well as the second site (His52). The former indeed forms the structural core, while the latter interacts with Phe57 of the C-terminal loop and contributes to restricting the conformation of the C-terminal loop to some extent (Fig. 3A).

The structure is indeed very similar to those of *Arabidopsis* SPL4- and SPL7-SBPs, except that SPL12-trSBP lack most of the C-terminal loop including one of the zinc-coordinating residues at the second binding pocket, Cys64 (Fig. 3B–D). Most of the hydrophobic interactions listed above were also conserved. Therefore, it is concluded that the second zinc-binding site is not essential in the maintenance of the SBP-domain structure. Considering the previous observation that chelating the two zinc ions leads to the structural unfolding of the SBP domain [6], the first zinc-binding site should be essential in the folding of the structure.

In the previous report, we have suggested that the SBP domain structure can be divided into two subdomains (residues 1–32 and 34–65), each containing a single zinc-binding pocket [6]. At the same time, we have also pointed out that these putative subdomains are tightly packed to each other, through interactions of hydrophobic residues, such as Val6, Val25, Phe/Tyr44, and Phe51, and that SBP domain should thereby behave essentially as a single domain, which is fully consistent with the present observations.

3.4. Role of the second zinc-binding site in the DNA binding

In the previous study, we have demonstrated the sequence-specific DNA-binding activities of the SBP domains of *Arabidopsis* SPL4 and SPL7 by measurement of surface plasmon resonance (SPR) [6]. Here, we tested the ability of the two SPL12 SBP-fragments by the same method (Fig. 4). SPL12-flSBP binds to a double-stranded DNA containing the consensus sequence of the SBP-binding sites, TNCGTACAA, where *N* stands for any base [2], with equilibrium binding constants of $>5\times10^8$, 1.3×10^8, and $3.2\times10^7\ M^{-1}$ at KCl concentrations of 100, 200 and 300 mM, respectively. The response ratio of the maximal binding of the protein to the DNA immobilized on the SPR sensor chip suggests that SPL12-flSBP binds to this DNA at a stoichiometry of 1:1. SPL12-flSBP binds much more weakly to a DNA of an unrelated sequence (estimated binding constant is $2.3\times10^6\ M^{-1}$ at 100 mM KCl concentration and $<10^5\ M^{-1}$ at 300 mM KCl concentration), indicating its ability of sequence-specific binding. These observations are largely consistent with the previous observations for SPL4-SBP [6].

In contrast, SPL12-trSBP did not bind to the DNA, significantly (Fig. 4B). This indicates that the C-terminal truncated region that contains nine conserved basic residues, as well as one of the zinc-coordinating residue, is essential in the DNA binding. In our previously constructed model of the protein-DNA complex that was consistent with an NMR titration experiment, the C-terminal basic loop deeply enters the major groove of DNA and contact bases [6]. It was also reported that the truncation behind Arg74 of SPL1 impairs the DNA binding [7]. All of these observations including the present results are consistent with one another.

It has been reported that mutations at four zinc-coordinating residues, Cys9, His29, Cys45, and Cys64 result in complete loss of the DNA binding [7]. The first two of these belong to the first zinc-binding site and the mutations are likely to lead

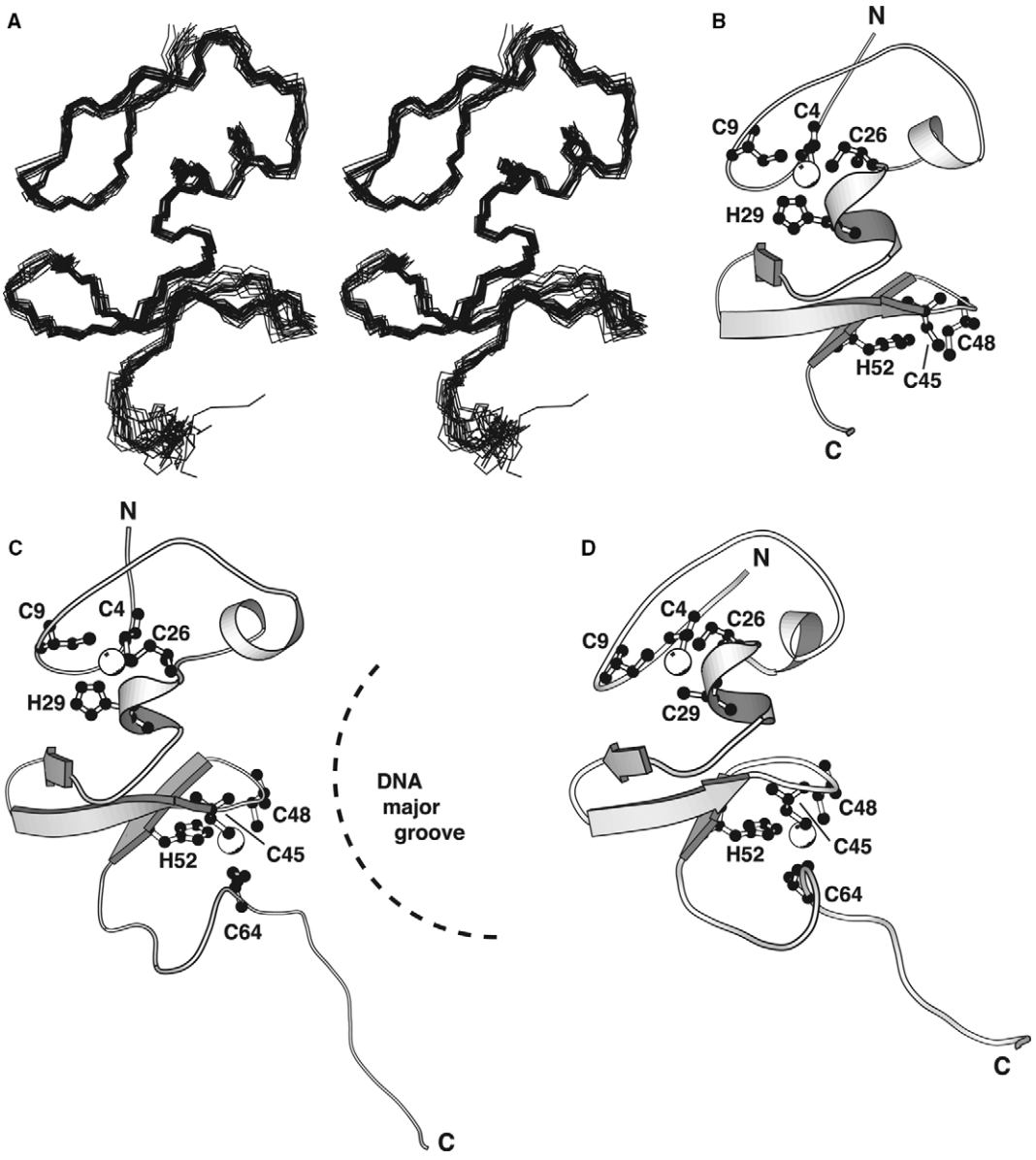

Fig. 3. Solution structures of SBP domains. The ensemble of the selected structures (A) and ribbon diagrams of the minimized mean structures (B) of SPL12-trSBP, and previously determined structures of the SBP domains of *Arabidopsis* SPL4 (C) and SPL7 (D) are shown. In (B)–(D), zinc ions and zinc-coordinating residues are presented by the spheres and the ball-and-stick presentations, respectively. The dashed curve in (C) schematically represents the DNA major groove in the structural model of the protein–DNA complex, in which the flexible C-terminal loop fits into the groove more closely [6]. The residue numbers used are for the SBP domain as aligned in Fig. 1A and not for the full-length proteins. The figures were produced by Molscript [21].

to structural unfolding, which naturally cause loss of the DNA binding. The last two belong to the second zinc-binding site, the mutations of which should not cause structural unfolding, according to the present results. It is likely, therefore, that the second Zn^{2+} ion is required for the DNA binding in more direct manner. In the previous report, we identified a large continuous area of positively charged surface, which consisted of all the conserved basic residues of the SBP domains, including the highly basic C-terminal loop. This surface possesses a curvature suitable for fitting into the DNA major groove, as schematically shown in Fig. 3C. From a structural point of view, the second zinc-binding site appears to be essential in forming this curvature, by guiding the C-terminal loop correctly. It should be also pointed out that a reanalysis of the previously constructed coordinates of the complex model [6] revealed a close proximity of the second Zn^{2+} ion to two phosphate group oxygens of DNA (distances <5 Å) (data not shown), presumably contributing to the intermolecular electrostatic attraction.

It is very interesting that mutation of His52 at the second zinc-binding site only partially impairs the DNA binding [7]. This appears to be consistent with the present observation that the second zinc-binding site is not important in folding of the SBP domain. According to the above discussions, we suggest a possibility that the mutant at His52 still binds a Zn^{2+} ion at the second site at least in the complex with DNA that attracts positively charged Zn^{2+} ion. Consequently, the C-terminal basic loop can be correctly guided to the DNA major groove by coordination of Cys64 to the Zn^{2+} ion, which is still impossible

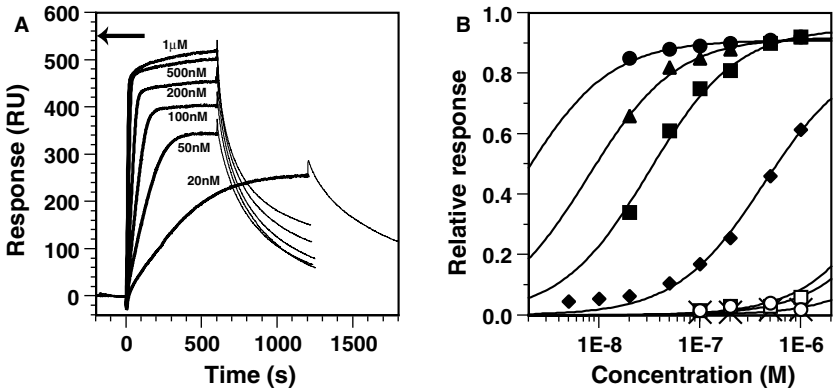

Fig. 4. DNA binding of SPL12-SBP fragments observed by surface plasmon resonance (SPR). (A) SPR difference sensorgrams (the responses in the control flow cell were subtracted) for binding of SPL12-flSBP to a 17mer double-stranded DNA (5′-GACGTCCGTACAACAAG-3′/5′-CTTGTTGTACGGACGTC-3′; the consensus sequence of the SBP-binding sites [2] is underlined), where the protein concentrations are 20 nM–1 μM, as indicated beside the sensorgram lines. The protein solutions were injected during a period of 0–1200 s for 20 nM or 0–600 s for 50 nM–1 μM, where the lines were rendered bold. The arrow indicates the maximum response value expected when the protein molecules bind to all the immobilized DNA molecules at 1:1 binding stoichiometry. (B) Equilibrium response values relative to the expected maximum values at a 1:1 stoichiometry, as functions of the protein concentration. Presented are the binding profiles of SPL12-flSBP (closed symbols) and SPL12-trSBP (open symbols) to the double-stranded 17mer DNA (as above), in the presence of 100 (circles), 200 (triangles; not performed for SPL12-trSBP), or 300 (squares) mM KCl. Those of SPL12-flSBP to another 18mer DNA with unrelated sequence, [5′-GGGCATTTATCTTGAATC-3′/5′-GATTCAAGATAAATGCCC-3′], in the presence of 100 (closed diamonds) or 300 (crosses) mM KCl are also shown. Fitting curves to the simple 1:1 binding model are shown.

for the mutant at Cys64. Coordination of three Cys/His residues to a Zn^{2+} ion has been indeed reported, for example, on the catalytic site of carbonic anhydrase, where a water molecule also participates as the fourth ligand [18]. To prove this hypothesis, however, number of bound Zn^{2+} ions of the His52 mutant in the complex with DNA should be determined in the future.

A recent report [19] proposed models for the mechanism of the copper-responsive interference of transcription activation by *Chlamydomonas* copper response regulator 1 (CRR1) that contains a SBP domain. One of the proposed models involves the SBP domain: a Cu^{2+} ion binds to the SBP domain and induces changes in its tertiary structure, resulting in the loss of the DNA-binding activity. It was suggested in the report that this structural change includes rearrangement of the zinc-binding sites, which would lead to replacement of one of the bound Zn^{2+} ions by a Cu^{2+} ion. Considering the present result showing that only the first zinc-binding site is necessary for maintaining the structure, we propose that the Cu^{2+} ion binds to the Cys/His residues at the second binding site, resulting in the replacement of the Zn^{2+} ion. Since the geometry of the four-ligand coordination to a Cu^{2+} ion is square planar but not tetrahedral (see e.g., PDB entry 1A8 V: Rho transcription termination factor RNA-binding domain), replacement of the ion should cause large change in the relative positions of the ligands, which would lead to exchange of one or two ligand residues of the four. This probably forces the bound ion unable to correctly guiding the C-terminal basic loop to the DNA groove, and thereby interferes the DNA binding. Since the amino acid sequence of this *Chlamydomonas* SBP domain is highly similar to those of *Arabidopsis* ones [7], the presumable ion exchange would occur also for the Arabidopsis proteins. Along with the progress in the functional analyses of *Arabidopsis* proteins, an SBP protein involved, e.g., in the environmental stress response, being regulated by the ion exchange mechanism, would be identified in the future.

Acknowledgements: The authors thank S. Watanabe, N. Matsuda, Y. Motoda, Y. Fujikura, Y. Miyata, K. Hanada, A. Kobayashi, M. Ikari, F. Hiroyasu, Y. Nishimura, M. Sato, M. Hirato, Y. Tsuboi, T. Harada, Y. Ishizuka, and H. Hamana at RIKEN for technical assistance, H. Yamaguchi, and K. Chiba-Kamoshida at AIST for helpful discussion, and M. Tateno at Tsukuba University for providing the coordinates of the complex model. This work was supported by the RIKEN Structural Genomics/Proteomics Initiative (RSGI) and the National Project on Protein Structural and Functional Analyses, Ministry of Education, Culture, Sports, Science and Technology.

References

[1] Klein, J., Saedler, H. and Huijser, P. (1996) A new family of DNA-binding proteins includes putative transcriptional regulators of the *Anthirrhinum majus* floral meristem identity gene SQUAMOSA. Mol. Gen. Genet. 259, 7–16.
[2] Cardon, G., Höhmann, S., Klein, J., Nettesheim, K., Sardler, H. and Huijser, P. (1999) Molecular characterisation of the *Arabidopsis* SBP-box genes. Gene 237, 91–104.
[3] Cardon, G., Höhmann, S., Nettesheim, K., Sardler, H. and Huijser, P. (1997) Functional analysis of the *Arabidopsis thaliana* SBP-box gene SPL3: a novel gene involved in the floral transition. Plant J. 12, 367–377.
[4] Unte, U.S., Sorensen, A.-M., Pesaresi, P., Gandikota, M., Leister, D., Saedler, H. and Huijser, P. (2003) *SPL8*, an SBP-box gene that affects pollen sac development in Arabidopsis. Plant Cell 15, 1009–1019.
[5] Stone, J.M., Liang, X.L., Nekl, E.R. and Stiers, J.J. (2005) Arabidopsis AtSPL14, a plant-specific SBP-domain transcription factor, participates in plant development and sensitivity to fumonisin B1. Plant J. 41, 744–754.
[6] Yamasaki, K., Kigawa, T., Inoue, M., Tateno, M., Yamasaki, T., Yabuki, T., Aoki, M., Seki, E., Matsuda, T., Nunokawa, E., Ishizuka, Y., Terada, T., Shirouzu, M., Osanai, T., Tanaka, A., Seki, M., Shinozaki, K. and Yokoyama, S. (2004) A novel zinc-binding motif revealed by solution structures of DNA-binding domains of *Arabidopsis* SBP-family transcription factors. J. Mol. Biol. 337, 49–63.
[7] Birkenbihl, R.P., Jach, G., Saedler, H. and Huijser, P. (2005) Functional dissection of the plant-specific SBP-domain: overlap of the DNA-binding and nuclear localization domains. J. Mol. Biol. 352, 585–596.

[8] Seki, M., Narusaka, M., Kamiya, A., Ishida, J., Satou, M., Sakurai, T., Nakajima, M., Enju, A., Akiyama, K., Oono, Y., Muramatsu, M., Hayashizaki, Y., Kawai, J., Carninci, P., Itoh, M., Ishii, Y., Arakawa, T., Shibata, K., Shinagawa, A. and Shinozaki, K. (2002) Functional annotation of a full-length *Arabidopsis* cDNA collection. Science 296, 141–145.

[9] Kigawa, T., Yabuki, T., Yoshida, Y., Tsutsui, M., Ito, Y., Shibata, T. and Yokoyama, S. (1999) Cell-free production and stable-isotope labelling of milligram quantities of proteins. FEBS Lett. 442, 15–19.

[10] Kigawa, T., Yabuki, T., Matsuda, N., Matsuda, T., Nakajima, R., Tanaka, A. and Yokoyama, S. (2004) Preparation of *Escherichia coli* cell extract for highly productive cell-free protein expression. J. Struct. Funct. Genom. 5, 63–68.

[11] Yokoyama, S., Hirota, H., Kigawa, T., Yabuki, T., Shirouzu, M., Terada, T., Ito, Y., Matsuo, Y., Kuroda, Y., Nishimura, Y., Kyogoku, Y., Miki, K., Masui, R. and Kuramitsu, S. (2000) Structural genomics projects in Japan. Nat. Struct. Biol. 7 (Suppl.), 943–945.

[12] Anderegg, G. (1963) Komplexone XXXIII. Reaktionsenthalpie und-entropie bei der buildung der metallkomplexe von äthylen-diamin- und diaminocyclohexan-tetraessigsäure. Helv. Chim. Acta 46, 1833–1842.

[13] Wüthrich, K. (1986) NMR of Proteins and Nucleic Acids, Wiley, New York.

[14] Nilges, M., Clore, G.M. and Gronenborn, A.M. (1998) Determination of the three-dimensional structures of proteins from interproton distance data by dynamic simulated annealing from a random array of atoms. FEBS Lett. 239, 129–136.

[15] Brünger, A.T., Adams, P.D., Clore, G.M., DeLano, W.L., Gros, P., Grosse-Kunstleve, R.W., Jiang, J.S., Kuzewski, J., Nilges, M., Pannu, N.S., Read, R.J., Rice, L.M., Simonson, T. and Warren, G.L. (1998) Crystallography & NMR system: a new software suite for macromolecular structure determination. Acta Crystallogr. D Biol. Crystallogr. 54, 905–921.

[16] Fersht, A. (1984) Enzyme Structure and Mechanism, 2nd edn, W.H. Freeman and Company, New York, p. 3.

[17] Laskowski, R.A., Rullman, J.A.C., MacArthur, W.M., Kaptein, R. and Thornton, J.M. (1996) AQUA and PROCHECK-NMR: programs for checking the quality of protein structures solved by NMR. J. Biol. NMR 8, 477–486.

[18] Eriksson, A.E., Jones, T.A. and Lijas, A. (1988) Refined structure of human carbonic anhydrase II at 2.0 Å resolution. Proteins: Struct. Funct. Genet. 4, 274–282.

[19] Kropat, J., Totty, S., Birkenbihl, R.P., Depége, N., Huijser, P. and Merchant, S. (2005) A regulator of nutritional copper signalling in Chlamydomonas is an SBP domain protein that recognizes the GTAC core of copper response element. Proc. Natl. Acad. Sci. USA 102, 18730–18735.

[20] Thompson, J.D., Gibson, T.J., Plewniak, F., Jeanmougin, F. and Higgins, D.G. (1997) The CLUSTAL-X windows interface: flexible strategies for multiple sequence alignment aided by quality analysis tools. Nucl. Acids Res. 25, 4876–4882.

[21] Kraulis, P.J. (1991) MOLSCRIPT: A program to produce both detailed and schematic plots of protein structures. J. Appl. Crystallogr. 24, 946–950.